
Effect of Reynolds Number on the Mixing Layer of an Axisymmetric Jet

Md. Tazul Islam

Mech. Engg. Dept.,
BIT, Chittagong, Bangladesh

M. A. Taher Ali

Mech. Engg. Dept., BUET,
Dhaka-1000, Bangladesh

Received : June 13, 1994

Accepted : Oct. 15, 1995

Abstract: An axisymmetric jet surrounded by free shear layer in the near field has been investigated experimentally for Re_d range 3.4×10^4 to 1×10^5 . The initial condition was taken at 0.5 mm downstream from the nozzle tip. Remarkable effect of Reynolds number was found for shifting of geometric virtual origin, extend of potential core length and partial self-preservation zone. Reynolds number greater than 5.3×10^4 has found negligible effect on entrainment rate.

Keywords : *Axisymmetric jet, Mixing layer.*

INTRODUCTION

Axisymmetric free jet has been studied extensively over a period of many years and from many perspectives. Visual observations made by Reynolds [1] and others showed many different types of flow phenomena which depends primarily on the jet Reynolds number. For a given set of initial boundary conditions, the mean and turbulent characteristics of the initial boundary layer as well as the Reynolds number determine the evolution of mixing layer of a free jet. Lemieux and Oosthuizen [2] found from their measurements in a plane jet that the spread rate of the jet affected slightly by the discharge Reynolds number, but the turbulent stress level was strongly dependent upon the Reynolds number. Hussain and Zedan [3] showed from their experimental results in an axisymmetric jet that the spread rate, similarity parameter, peak turbulent intensity in the self-preserving region were essentially independent of Reynolds number, but depends on whether the initial boundary layer was laminar or turbulent. They also found that the geometric virtual origin as well as the distance required for attainment of self-preservation depends noticeably and systematically on Reynolds number. The shifting of geometric virtual origin for Reynolds number also investigated by Selim and Ali [4] and others [5,6]. Gama et al. [6] also found that the achievement of self-preservation decreased with the increase of Reynolds number. Ricou & Spalding [7] showed that for Reynolds number greater than 3×10^4 , the entrainment rate (in the developed region) was independent of Reynolds number and strongly dependent upon the axial distance with non-linear relationship. Hill [8] found that the entrainment rate (in the

near field) was independent on the exit Reynolds number for values greater than 6×10^4 and was strongly dependent upon the axial distance. Trabold et al. [9] showed that this independent of Reynolds number in the initial region was greater than 2×10^4 , but moderate Reynolds number effect was evidence in the fully developed region for less than 2×10^4 . This effect of Reynolds number on entrainment rate was also investigated by Hussain and Clark [10] and found that less influence.

The objectives of this study were investigated the flow characteristics of an axisymmetric jet in the near field for Reynolds number (based on nozzle diameter) range 3.4×10^4 to 1×10^5 , which includes: measuring the axial mean velocity in the free shear layer at different axial downstream location from the nozzle exit. Some other properties were calculated from the mean velocity profiles such as entrainment rate, viscous and Reynolds shear stresses.

EXPERIMENTAL SET-UP AND METHODOLOGY

The experiment was carried out in a air jet facility (Fig.1a) consisted of two settling chambers, fan unit, flow controller diffusers, an excitation chamber and flow nozzle. The air supply in the system was provided by fan unit consists of two wooden aerofoil axial flow fans one with fixed speed motor and other with variable speed motor. The overall length of the set-up was 8.1 m.

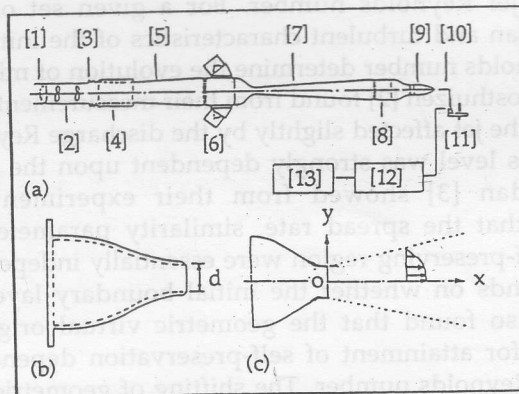


Fig. 1 : a) Experiment Set-up; [1] Flow controller, [2] Fan section, [3] Vibration Isolator, [4] Silencer box, [5] Diffuser-1, [6] Excitation and settling chamber-1, [7] Diffuser-2, [8] Settling chamber-2, [9] Test nozzle, [10] Pitot static tube, [11] Traversing mechanism, [12] Pressure transducer, [13] Microvoltmeter. b) Test Nozzle. c) Co-ordinate system.

Air enters to the fan unit through butterfly valve which controls the air flow. A silencer was fitted at the discharge of the fan to reduce noise generated at the fan discharge. Flow from the silencer enters to the settling chamber through a 6° diffuser, in this chamber the flow straightener and wire screen nets were used to straighten the flow as well as to breakdown large eddies generated at the fan discharge. Flow then enters to the excitation chamber, here two loudspeakers (200 watt each) were placed opposite to each other at an angle 45° with the central axis (for future provision of upstream excitation measurements). Air from this chamber flows to the second settling chamber through a nozzle and a second diffuser, here also straightener and wire screen nets were used for ensuring axial flow free of large eddies which may be generated in the upstream side of the flow. Finally air then discharges through a circular convergent parabolic nozzle (Fig.1b).

The experiment was done in the near field of the circular jet by the application of United sensor pitot-static tube along with Furnace control pressure transducer and Kiethly data logger for measuring velocity head. The pitot-static tube was traversed with smallest division 0.01 mm with the help of a Mitutoyo three coordinate (x,y & z) traversing mechanism. All raw data found from data logger in milli volt, were converted to velocity (m/s) by the calibration equation

$$u = \sqrt{16.618 (0.111 + 0.248 M)}$$

The exit centerline of the nozzle in the direction of the flow was taken as positive x-axis and radial distance pointing upward as positive y-axis (Fig.1c). All differential form of equations were solved by finite-difference method and integral form of equations by trapezoidal method. The exit condition was taken at 0.5 mm downstream from the nozzle tip. The measurements were taken upto y_{\max} in the initial mixing region and in the centerline upto $x/d=8$ downstream distance from the nozzle exit.

RESULTS AND DISCUSSION

Exit boundary layer profiles at Reynolds number $Re_d=3.4 \times 10^4$, 5.3×10^4 , 7.6×10^4 and 1×10^5 are shown in Fig.2. The Blasius profile is also plotted in the same figure to ascertain the initial boundary layer condition. The measurement shows

that the initial boundary layer profiles at $Re_d=3.4 \times 10^4$ and 5.3×10^4 lies on the Blasius profile having shape factor 2.55 and 2.62 respectively. But at $Re_d=7.6 \times 10^4$ and 10×10^4 the shape factor are 1.73 and 1.5 which is closed to 1.4. So it may be assumed that the initial boundary layer profile is laminar in the range of $Re_d=3.4 \times 10^4$ to 5.3×10^4 and turbulent in the range $Re_d=7.6 \times 10^4$ to 10×10^4 .

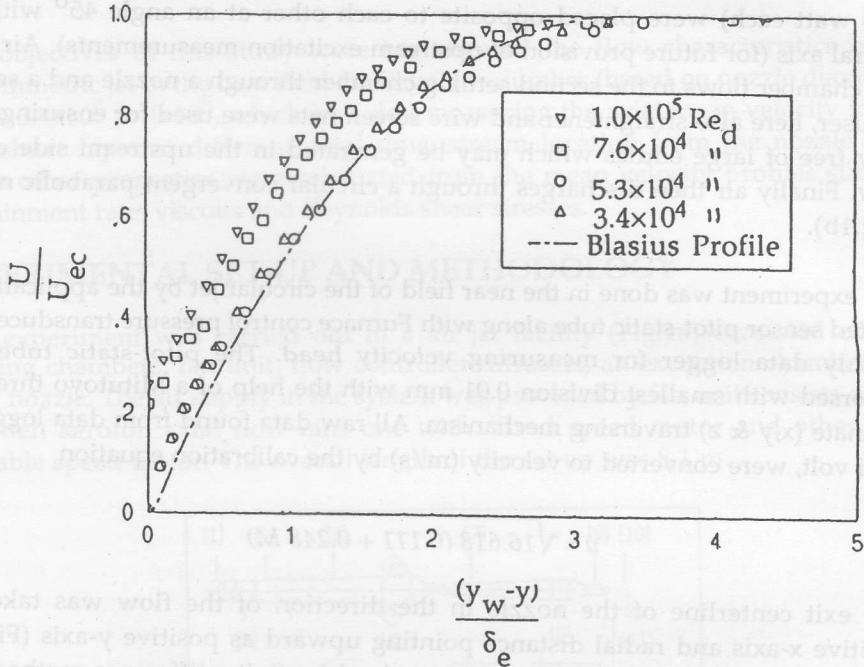


Fig. 2 : Initial Boundary Layer Profiles.

Iso-velocity lines of the mixing layer are shown in Fig.3, it is seen that the effect of Reynolds number on outer edge ($U/U_{ec}=0.1$ line) is significant and the shear layer increased with increasing Reynolds number but for half-width mixing layer ($U/U_{ec}=0.5$ line) have negligible effect. Further the intersection of inner edge shear layer ($U/U_{ec}=0.95$ line) with central axis is different for different Reynolds number, which indicates that the length of potential core is increased with the increase of Reynolds number. The conclusion also drawn by Gama et al.[6].

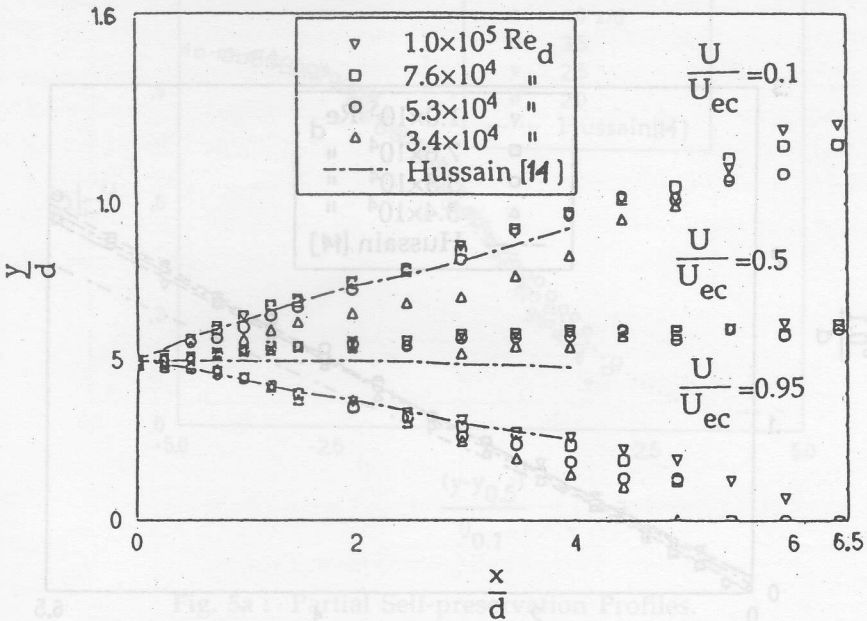


Fig. 3 : Iso-velocity Lines.

The distribution of shear layer momentum thickness is presented in the Fig.4, it is seen that $\theta_{0.1}$ varied linearly with the downstream distance. According to the equation, $\theta_{0.1}/d=k(x/d+c)$ [11], (where, k is the slope of the profile and c is the geometric virtual origin) the geometric virtual origins are found at $x/d=+0.016, +0.007, -0.151$ and -0.266 for $Re_d=3.4 \times 10^4, 5.3 \times 10^4, 7.6 \times 10^4$ and 10×10^4 respectively. From these results it may be said that the geometric virtual origin is at downstream of the nozzle tip for initial laminar boundary layer and for turbulent it is at upstream. The similar conclusion also drawn by Crow and Champagne [12]. It is also seen that due to the increase of Reynolds number the location of virtual origin moves from downstream to upstream. This significant effect of Reynolds number on shifting of geometric virtual origin was also found by others [3,13].

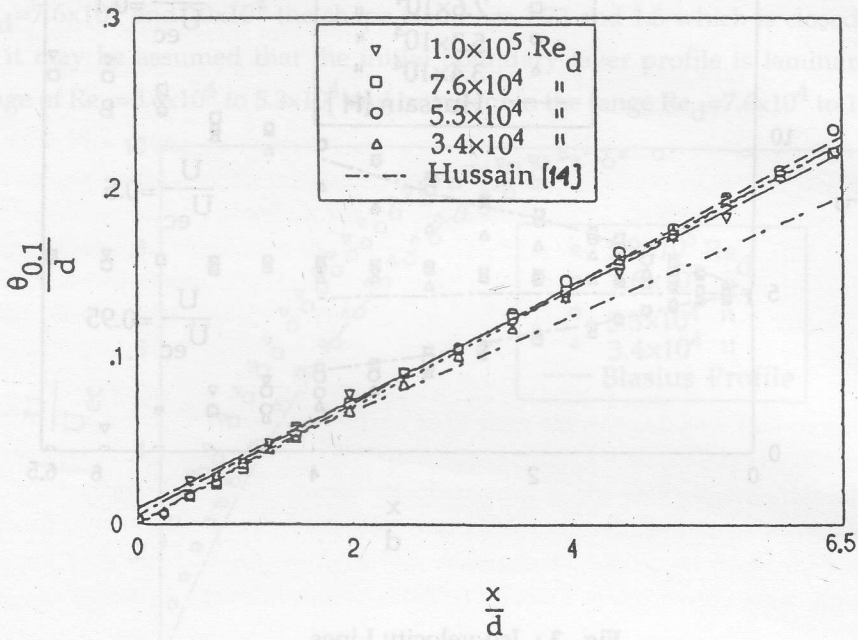


Fig. 4 : Shear Layer Momentum Thickness.

Partial self-preservation profiles of mean velocity are presented in Fig.5a,b,c. The self-preservation variables $(y-y_{0.5})/\theta_{0.1}$ is considered in this present measurements. The profiles are found close agreement with Hussain and Clark [14]. The self-preserving zone are extended from $x/d=2$ to 4, 1 to 5 and 1 to 5.5 at $Re_d=5.3 \times 10^4$, 7.6×10^4 and 1×10^5 respectively, after that the jet losses its self-preservation due to the transition or absence of the potential core. It may be concluded that the self-preservation zone is increased due to increase of the Reynolds number. Similar results also found by Bradshaw [5].

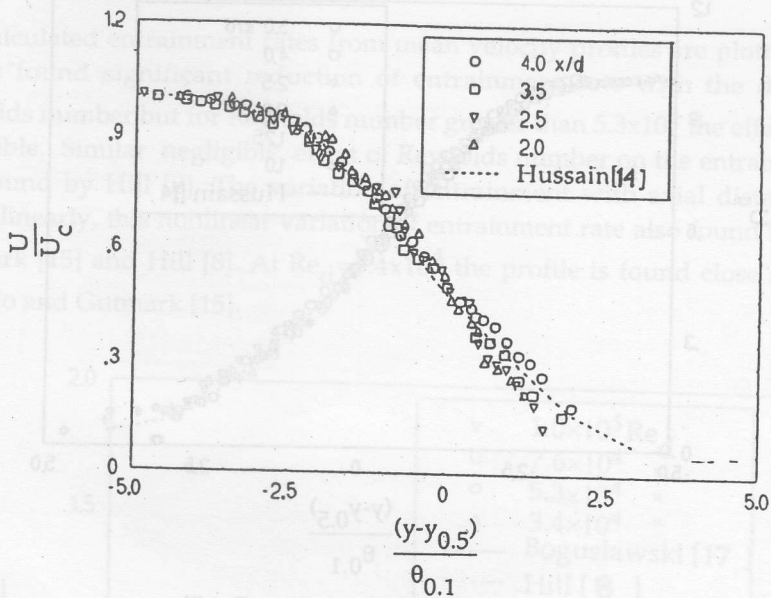


Fig. 5a : Partial Self-preservation Profiles.

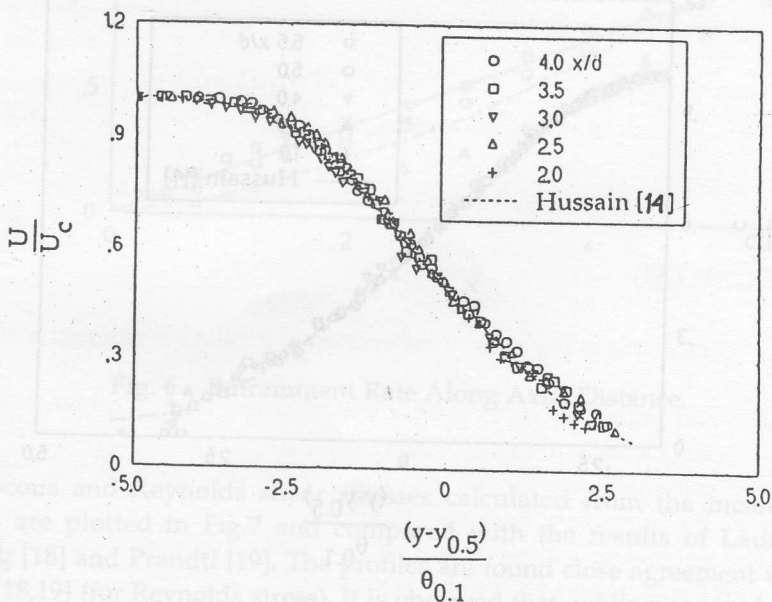


Fig. 5b : Partial Self-preservation Profiles.

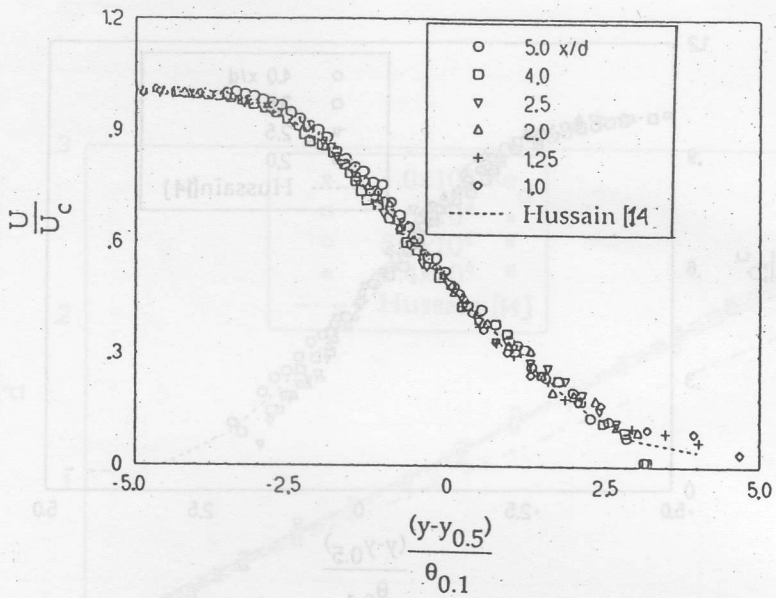


Fig. 5c : Partial Self-preservation Profiles.

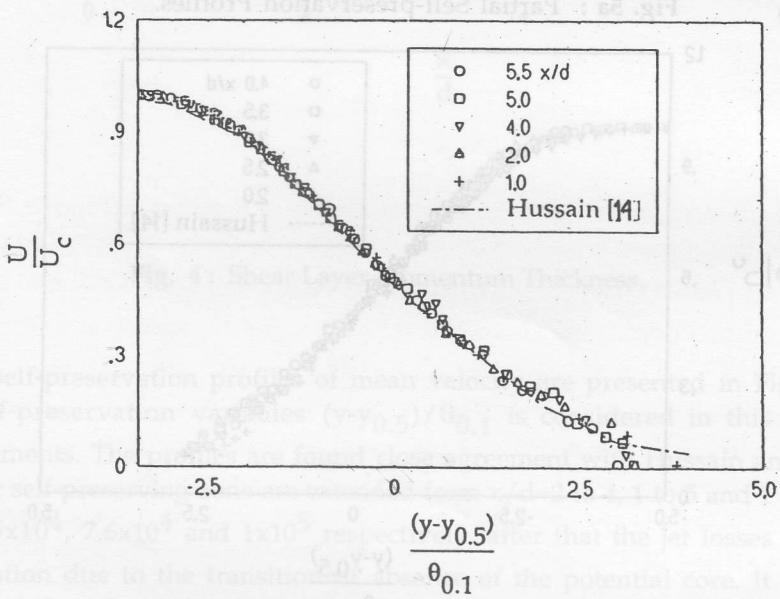


Fig. 5d : Partial Self-preservation Profiles.

The calculated entrainment rates from mean velocity profiles are plotted in Fig.6 and is found significant reduction of entrainment rate with the decrease of Reynolds number but for Reynolds number greater than 5.3×10^4 the effect is found negligible. Similar negligible effect of Reynolds number on the entrainment rate also found by Hill [8]. The variation of entrainment with axial distance is not found linearly, this nonlinear variation of entrainment rate also found by Ho and Gutmark [15] and Hill [8]. At $Re_d = 3.4 \times 10^4$ the profile is found close agreement with Ho and Gutmark [15].

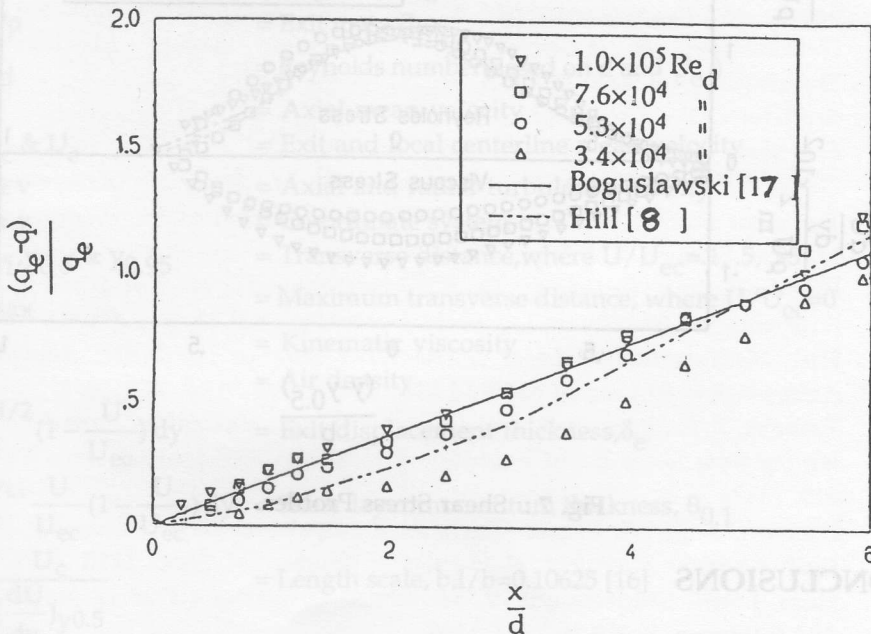


Fig. 6 : Entrainment Rate Along Axial Distance.

The viscous and Reynolds shear stresses calculated from the mean velocity profiles are plotted in Fig.7 and compared with the results of Launder and Spalding [18] and Prandtl [19]. The profiles are found close agreement with their results [18,19] (for Reynolds stress). It is observed that, while viscous shear stress decreases corresponding Reynolds shear stress is increased. This may happen by continuous transfer of energy from the mean flow field to the generation of

turbulence. Due to the change of Reynolds number the shear stress profiles are affected, which is pronounced for viscous shear stress. The decay rate of viscous shear stress is decreased with the increase of Reynolds number.

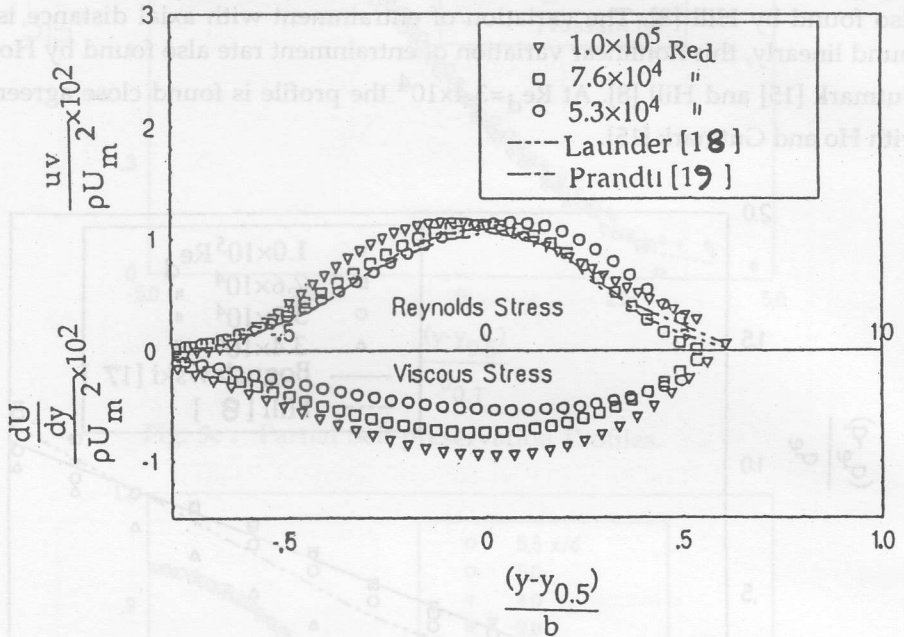


Fig. 7 : Shear Stress Profiles.

CONCLUSIONS

The major conclusions of the present experimental results are summarized below.

1. The exit boundary layer profile was changed from laminar to turbulent with the increase of Reynolds number.
2. The potential core length and the self-preserving zone were increased with the increase of Reynolds number.
3. The geometric virtual origin of the shear layer was shifted upstream with the increase of Reynolds number.

4. The effect of Reynolds number was remarkable on viscous shear stress and the entrainment rate has negligible effect when the Reynolds number is greater than 5.3×10^4 .

NOMENCLATURE

d	= Exit diameter of the nozzle
l	= Prandtl's mixing length
M	= Milli volt
o	= Physical origin
q_e/ρ	= Exit mass flux
Re_d	= Reynolds number(based on d and U_{ec})
U	= Axial mean velocity
U_{ec} & U_c	= Exit and local centerline mean velocity
u & v	= Axial and radial turbulent intensity
x & y	= Co-ordinate system
$y_{0.1}, y_{0.5}$ & $y_{0.95}$	= Transverse distance, where $U/U_{ec} = .1, .5, .95$
y_{max}	= Maximum transverse distance, where $U/U_{ec} = 0$
v	= Kinematic viscosity
ρ	= Air density
$\int_0^{d/2} (1 - \frac{U}{U_{ec}}) dy$	= Exit displacement thickness, δ_e
$\int_0^{y_{0.1}} \frac{U}{U_{ec}} (1 - \frac{U}{U_{ec}}) dy$	= Shear layer momentum thickness, $\theta_{0.1}$
$\frac{U_c}{(\frac{dU}{dy})_{y_{0.5}}}$	= Length scale, $b, l/b = 0.10625$ [16]
$v \frac{dU}{dy}$	= Viscous shear stress
$\rho l^2 \left \frac{dU}{dy} \right \frac{dU}{dy}$	= Reynolds shear stress, θ_{uv}
$2\pi U_{ec} \int_0^{y_{max}} \frac{U}{U_{ec}} y dy$	= Mass flux, q/ρ

REFERENCES

- [1] Reynolds, A. J., *Observation of a Liquid into Liquid Jet*, Journal of Fluid Mechanics, Vol. 14, p. 522, 1962.
- [2] Lemieux, G. P. and Oosthuizen, P. H., *Experimental Study of the Behavior of Plane Turbulent Jets at Low Reynolds Numbers*, AIAA Journal, Vol. 23, p. 1845, 1985.
- [3] Hussain, A. K. M. F. and Zedan, M. F., *Effects of the Initial Condition on the Axisymmetric Free Shear Layer: Effects of the Initial Momentum Thickness*, Physics of Fluids, Vol. 21, p. 1100, 1978.
- [4] Selim, M. A. and Ali, M. A. T., *Effect of Initial Conditions on Development of Axisymmetric Free Shear Layer*, Mechanical Engineering Research Bulletin, Vol. 11, p. 49, 1988.
- [5] Bradshaw, P., *The Effect of Initial Conditions on the Development of a Free Shear Layer*, Journal of Fluid Mechanics, Vol. 26, p. 226, 1966.
- [6] Gama, B. A., Ali, M. A. T. and Islam, A. K. M., *Study of Axisymmetric Turbulent Free Mixing Layer and Jet*, Indian Journal of Engineering and Material Science, Vol. 1, p. 246, 1994.
- [7] Ricou, P. and Spalding, D. B., *Measurements of Entrainment by Axisymmetric Jets*, Journal of Fluid Mechanics, Vol. 11, p. 21, 1961.
- [8] Hill, *Measurement of Local Entrainment Rate in the Initial Region of Axisymmetric Jet*, Journal of Fluid Mechanics, Vol. 51, p. 773, 1972.
- [9] Trabold, T. A., Esen, E. B. and Obot, N. T., *Entrainment by Turbulent Jets Issuing from Sharp-Edged Inlet Round Nozzle*, ASME Journal, Vol. 109, p. 413, 1987.
- [10] Hussain, A. K. M. F. and Clark, A. R., *Upstream Influence on the Near Field of a Plane Turbulent Jet*, Physics of Fluids, Vol. 20, p. 1416, 1977.
- [11] Flora, J. and Goldschmidt, V. M. *Virtual Origins of a Free Turbulent Jet*, AIAA Journal, Vol. 7, p. 2344, 1969.
- [12] Crow, S. C. and Champagne, F. H., *Orderly Structure in Jet Turbulence*, Journal of Fluid Mechanics, Vol. 48, p. 547, 1971.
- [13] Selim, M. A., *Flow Structure of the Circular Wedge Shaped Jet*, M. Sc. Thesis, BUET, Dhaka, 1988.
- [14] Hussain, A. K. M. F. and Clark, A. R., *On the Coherent Structure of the Axisymmetric Mixing Layer: a Flow Visualization Study*, Journal of Fluid Mechanics, Vol. 104, p. 263, 1981.

- [15] Ho, C. M. and Gutmark, E., *Vortex Induction and Mass Entrainment in a Small-Aspect-Ratio Elliptic Jet*, Journal of Fluid Mechanics, Vol. 179, p. 383, 1987.
- [16] Islam, S. M. N., *Prediction and Measurement of Turbulence in the Developing Region of Axisymmetric Isothermal Free Jets*, Ph. D Thesis, Windsor, Ontario, Chanda, 1979.
- [17] Boguslawski, L. and Popiel, CZ. O., *Flow Structure of the Free Round Turbulent Jet in the Initial Region*, Journal of Fluid Mechanics, Vol. 90, p. 531, 1979.
- [18] Launder, B. E. and Spalding, D. B., *The Numerical Calculation of Turbulent Flow*, Comp. Methods in Appl. Mech. and Eng., Vol. 3, p. 269, 1974.
- [19] Prandtl, L., *Bericht Unber Untersuchungen Zur Ausgebildeten Turbulenz*, ZAMM, Vol. 5, p. 136, 1925.

Received : July 14, 1994
Accepted : April 2, 1995

Keywords : Horizontal axis wind turbine, Wind shear, tower shadow.

INTRODUCTION

Modified Blade element theory or Strip theory which is used for the present analysis is the most frequently used theory for the design and performance analysis of a horizontal axis wind turbine. This section discusses the design of a horizontal axis wind turbine in which lift forces on airfoils are the driving forces. According to this theory, a rotor can be designed which produces an optimum power coefficient, to choose the lift and drag ratio of the profile constant and to keep it constant along the blade span. A second condition is that both a strongly varying blade twist are desired. This leads to a very complicated rotor blade configuration which can be expensive to manufacture and may not have structural integrity. In this paper, it is shown that it is possible to approach very closely the optimum blade configuration by taking a